A Journal of the Gesellschaft Deutscher Chemiker

Angewandte International Edition

GDCh

Chemie

www.angewandte.org

Accepted Article

Title: Pathway from N-alkylglycine to alkylisonitrile catalyzed by iron(II) and 2-oxoglutarate dependent oxygenases

Authors: Wei-Chen Chang, Tzu-Yu Chen, Jinfeng Chen, Yijie Tang, Jiahai Zhou, and Yisong Guo

This manuscript has been accepted after peer review and appears as an Accepted Article online prior to editing, proofing, and formal publication of the final Version of Record (VoR). This work is currently citable by using the Digital Object Identifier (DOI) given below. The VoR will be published online in Early View as soon as possible and may be different to this Accepted Article as a result of editing. Readers should obtain the VoR from the journal website shown below when it is published to ensure accuracy of information. The authors are responsible for the content of this Accepted Article.

To be cited as: *Angew. Chem. Int. Ed.* 10.1002/anie.201914896
Angew. Chem. 10.1002/ange.201914896

Link to VoR: http://dx.doi.org/10.1002/anie.201914896
http://dx.doi.org/10.1002/ange.201914896

WILEY-VCH

10.1002/anie.201914896

WILEY-VCH

COMMUNICATION

Pathway from N-alkylglycine to alkylisonitrile catalyzed by iron(II) and 2-oxoglutarate dependent oxygenases

Tzu-Yu Chen,[a],† Jinfeng Chen,[b],† Yijie Tang,[c] Jiahai Zhou,*[b] Yisong Guo,*[c] and Wei-chen Chang*[a]

We dedicate this paper to Professor Youli Xiao

[a] Tzu-Yu Chen, Dr. Wei-chen Chang
Department of Chemistry
North Carolina State University
Raleigh, NC 27695, U.S.A.
E-mail: wchang6@ncsu.edu
[b] Jinfeng Chen, Dr. Jiahai Zhou
State Key Laboratory of Bio-organic and Natural Products Chemistry, Center for Excellence in Molecular Synthesis
Shanghai Institute of Organic Chemistry, University of Chinese Academy of Sciences
Shanghai 200032, China
Email: jiahai@mail.sioc.ac.cn
[c] Yijie Tang, Dr. Yisong Guo
Department of Chemistry
Carnegie Mellon University
Pittsburgh, PA 15213, U.S.A.
Email: ysguo@andrew.cmu.edu

Supporting information for this article is given via a link at the end of the document.

Abstract: N-alkylisonitrile, a precursor to isonitrile-containing lipopeptides, is biosynthesized via decarboxylation-assisted -N≡C group (isonitrile) formation by using N-alkylglycine as the substrate. This reaction is catalyzed by iron(II) and 2-oxoglutarate (Fe/2OG) dependent enzymes. Distinct from typical oxygenation or halogenation reactions catalyzed by this class of enzymes, installation of the isonitrile group represents a novel reaction type for Fe/2OG enzymes that involves a four-electron oxidative process. Here we report the plausible mechanism of three Fe/2OG enzymes, Sav607, ScoE and SfaA, catalyzed isonitrile formation. The X-ray structures of iron loaded ScoE in complex with its substrate and the intermediate, along with biochemical and biophysical data reveal that -N≡C bond formation involves two cycles of Fe/2OG enzyme catalysis. The reaction starts with an Fe(IV)-oxo catalyzed hydroxylation. It is likely followed by decarboxylation-assisted desaturation to complete isonitrile installation.

Isonitrile-containing natural products have shown diverse biological activities.[1] Notably, two types of enzymes are involved in isonitrile formation (Scheme 1A). The first type employs an isonitrilase catalyzed condensation of the amine from the L-tyrosine/tryptophan with the carbonyl group of ribulose-5-phoshate.[2] The second type involves an iron(II) and 2-oxoglutarate (Fe/2OG) dependent enzyme catalyzed decarboxylation-assisted -N≡C group installation.[3] Analysis of the biosynthetic gene clusters responsible for the Fe/2OG enzyme catalyzed isonitrile formation revealed that the pathway involved in isonitrile-containing peptides production is conserved in pathogenic mycobacteria including *Mycobacterium tuberculosis*, and *M. marinum*. Related operons are also found in the phylum of Actinobacteria including *Streptomyces*.[1a, 3b]
The majority of Fe/2OG enzymes catalyze two-electron oxidative modifications that include hydroxylation, desaturation, epoxidation, halogenation and endoperoxide installation.[4] Addition of O_2 to the 2OG bound Fe(II) generates an Fe(IV)-oxo species which is used to activate the targeted C-H bond or acts as an oxygen atom donor to add onto the olefin moiety.[5] For those involving C-H activation, subsequent to hydrogen atom (H•) abstraction, an iron bound ligand transfers to the substrate radical to form the product and regenerates the Fe(II) (Scheme 1B).[4d, 6]

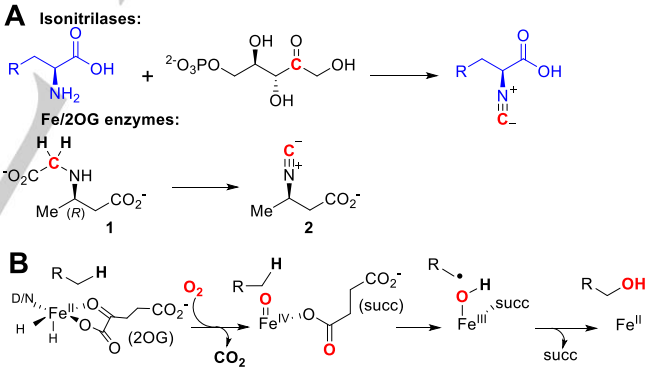

Scheme 1 A) Two different approaches used to install isonitrile. B) Fe/2OG enzyme catalyzed hydroxylation.

Differently, Fe/2OG enzyme catalyzed isonitrile formation is a four-electron oxidation and formally involves two C-H bond cleavage steps and a decarboxylation. Initial biochemical and structural characterizations of ScoE suggested that it is responsible for isonitrile formation.[3] The structure of zinc-bound ScoE indicates that it belongs to the cupin superfamily and has the 2-His-1-carboxylate triad as the iron-binding ligands.[3a] However, in this structure, the potential substrate-binding site was occupied by choline and the putative 2OG binding site was resided by acetate. Based on this structure, the reaction mechanism has been postulated to involve a hydroxylated imine species (**5**) that is likely generated via hydroxylation of the imine intermediate (**4**). Subsequent dehydration/decarboxylation of **5**

This article is protected by copyright. All rights reserved.

Accepted Manuscript

10.1002/anie.201914896

produces **2** (Scheme 2, pathway *i*). To date, this is the only experimentally characterized Fe/2OG isonitrile forming enzyme. To demonstrate a conserved approach may be utilized in introducing isonitrile functionality among isonitrile-containing peptides production, we use crystallographic, biochemical and biophysical methods to study three enzymes, Sav607, ScoE and SfaA, originated from *Streptomyces avermitilis*, *S. coeruleorubidus* and *S. thioluteus*, that are known, or are predicted, to catalyze isonitrile formation.[1a, 3b, 7]

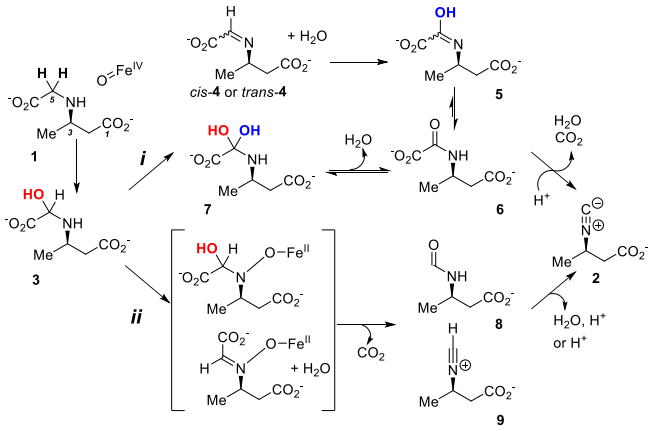

Scheme 2 Possible pathways for isonitrile formation. Starting from C5-hydroxylation, two pathways involving either second hydroxylation (pathway *i*) or decarboxylation-assisted desaturation (pathway *ii*) are proposed.

To overcome the reported issues of co-purification of zinc and choline with the protein, and the instability of the product that hamper direct mechanistic studies and structural analysis,[3a] we expressed and purified Sav607, ScoE and SfaA as metal-free proteins by chelating the co-purified metal using EDTA and then introduced Fe(II) in all experiments. A synthetic approach was developed to afford substrate (**1**), its isotope-labeled analogs ([5-$^{2}H_2$-**1**] and [5-^{13}C-**1**]), product (**2**), and mechanistic probes (cis-**4** and **6**) (detailed in Supporting Information (SI)).

We first carried out structural analysis. All three proteins were subjected to crystallization conditions, the ScoE and SfaA samples yielded diffraction quality crystals. Co-crystals of the substrate (**1**) and presumptive intermediate (**3**) bound ScoE were obtained by the sitting drop vapor diffusion technique (detailed in the SI). The structure of **1** and iron bound ScoE (ScoE•Fe•**1**) was then solved at a resolution of 2.18 Å. The overall structure contains 15 strands of β-sheet and 8 α-helices, eight of which forming a jellyroll motif (β3, β13, β5, β15, β4 and β12, β6, β14) (Figure 1A-B, S20 and Table S4). Dali search suggested the structure of ScoE resembles those of other Fe/2OG-enzymes such as CarC (PDB ID: 4oj8) and a putative dioxygenases (PDB ID: 4y0e), with Z-score of 20.0 and 26.7, respectively. In the structure of ScoE, the octahedron geometry of iron is bound by a 2-His-1-Asp facial triad (H132, D134, and H295). The fourth coordination site is occupied by a tartrate (TAR) molecule that is acquired during crystallization. The remaining two coordination positions are occupied by water molecules (W1 and W2). Significant electron density corresponding to **1** is visualized in the active site which has hydrogen-bonding interactions with Y101, K193, G128, Y96, Y135 and R310. Importantly, this structure implies the plausible reaction site where the C5 of **1** is 4.9 Å away from the iron with one of its hydrogens pointing toward to the iron. Compared to other Fe/2OG enzyme structures including TauD (PDB ID: 1os7), CarC (PDB ID: 4oj8), and PvcB (PDB ID: 3eat), a tartrate molecule is most likely positioned at the 2OG binding site. A putative quaternary complex structure of ScoE•Fe•2OG•**1** is modeled by docking the 2OG molecule into the substrate structure (Figure S20). In addition, a presumptive intermediate (**3**) bound ScoE structure with resolution of 2.17 Å was obtained (Figure 1B-C, S21, S22, S23 and Table S4). The electron density map of the structure clearly shows that this compound resembles the possible C5 hydroxylated product (**3**). Besides, the apo form of SfaA is highly similar to the structure of ScoE with rmsd of ~0.37 Å (Figure S24 and Table S4).

To establish the reaction pathway, the stoichiometry between 2OG and **1** was established. During Fe/2OG enzyme reaction, the Fe(II) is converted to the Fe(IV)-oxo species by reacting with O_2 and 2OG where 2OG is converted to succinate and CO_2 (Scheme 1B). Thus, the stoichiometry of 2OG and **1** can be established by quantifying succinate, and the isonitrile (**2**). Reactions with different amount of 2OG were carried out and analyzed by LC-MS (detailed in SI). As depicted in Figure S16, the peak with the same retention time and mass/charge (*m/z*) as the synthetic **2** accumulated when 2OG and O_2 were introduced. By quantifying succinate and **2**, the stoichiometry between succinate and **2** is determined as 2.3, 3.2 and 4.5 for SfaA, Sav607 and ScoE (Figure S17). Compared to SfaA, the higher uncoupling ratio observed in Sav607 and ScoE possibly arise from unproductive pathways. Similar uncoupling reactions have been observed in other Fe/2OG enzymes.[8] These results suggest that for one equivalent of **2** produced, two equivalents of 2OG are required. Thus, isonitrile group installation likely involves two sequential reactions.

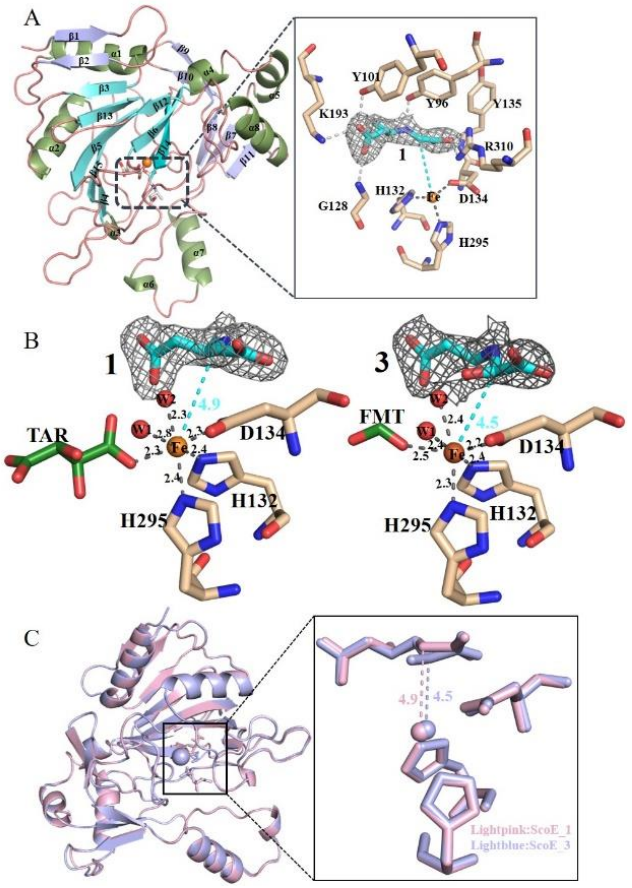

This article is protected by copyright. All rights reserved.

Accepted Manuscript

10.1002/anie.201914896

Figure 1. Crystal structures of ScoE. A) The overall structure of ScoE is shown in cartoon model, with the jellyroll motif colored in cyan. $2F_o$-F_c (light gray mesh, contoured at 1.0 σ) electron density map for **1**. Dashed lines illustrate hydrogen-bonding interactions involving **1** or bonds between the iron and its ligands. B) Active site of ScoE in the presence of **1** or **3**. Putative 2OG binding sites appear to be occupied by exogenous ligands colored in forest. The 2-His-1-Asp triad is shown in wheat stick format. Molecules **1** and **3** are colored in cyan, the electron density maps for **1** and **3** are shown in dark-gray mesh and contoured at 1.0 σ. Iron and waters are shown in orange and red sphere. Putative 2OG binding sites appear to be occupied by exogenous ligands (TAR or FMT) colored in forest. C) Superposition of ScoE•Fe•**1** and ScoE•Fe•**3**.

The presence of the C5-hydroxyalted compound (**3**) was established by the analysis of the ^{13}C-NMR spectrum of a sample prepared by reacting SfaA with 5-^{13}C-**1**, O_2 and 2OG (with the molar ratio of 5-^{13}C-**1** to 2OG of 1:1.5). The spectrum recorded under C-H decoupling mode exhibits a new peak at ~91 ppm that is not present in the absence of 2OG. The spectrum collected under C-H coupling mode reveals a doublet with a coupling constant of ~163 Hz (Figure 2 and S15). The chemical shift and the coupling pattern indicate that this carbon is connected to one proton, one carbon and two heteroatoms. This result is consistent with the ScoE•Fe•**1** structure where the C5-H of **1** points toward the iron and observation of the ScoE•Fe•**3** structure. When the ratio of 5-^{13}C-**1** to 2OG changed from 1:1.5 to 1:2.5, we observed a decrease of this species (**3**) and the appearance of the new peak centered at ~150 ppm. The NMR spectrum obtained under C-H coupling mode indicates that no proton is connected to this newly formed carbon. This newly formed peak has the same chemical shift as of the synthetic **2** (Figure S11 and S15). These results suggest that the isonitrile formation is at the expense of 2OG and **3** serves as the possible intermediate during isonitrile formation.

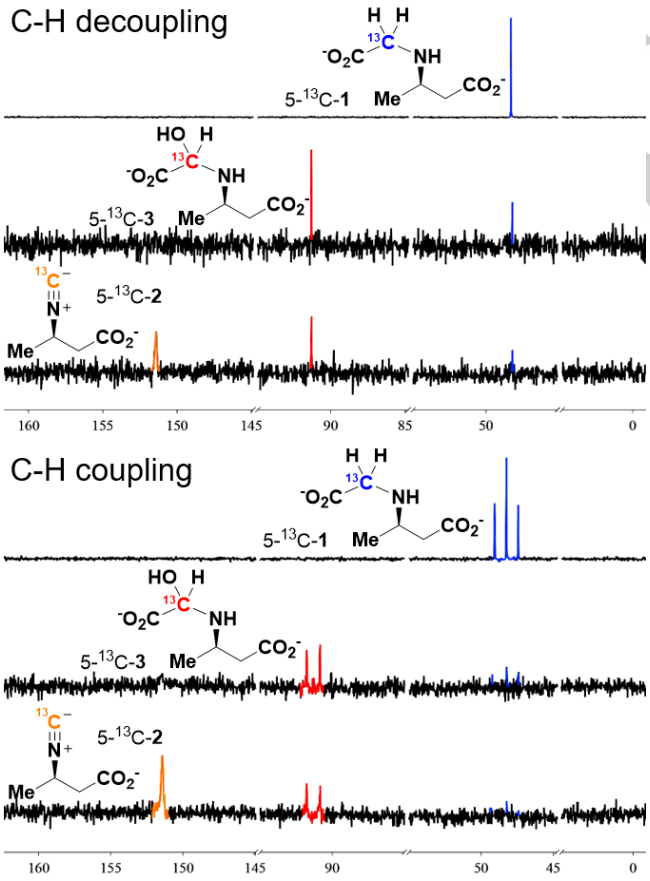

Figure 2. ^{13}C-NMR of SfaA catalyzed **2** formation under C-H decoupling and C-H coupling conditions. The top, middle and bottom traces represent the ^{13}C-NMR recorded with 5-^{13}C-**1** to 2OG ratio at 1:0, 1:1.5 and 1:2.5, respectively.

The requirement for the Fe(IV)-oxo, a.k.a. ferryl, species to cleave C5-H bond is verified by the Mössbauer analysis. Samples were prepared by mixing the SfaA•Fe(II)•2OG•**1** or 5-$^2H_2$-**1** complex (the quaternary complex) with oxygenated buffer and freeze quenching at various time points. The Mössbauer spectra of SfaA•Fe(II)•2OG•**1** or 5-$^2H_2$-**1** complex exhibit a quadrupole doublet with an isomer shift (δ) of 1.23 mm/s and quadrupole splitting (ΔE_Q) of 2.74 mm/s, which represents high-spin ferrous species (Figure 3, S19 and Table S1-S3). When 5-$^2H_2$-**1** was used, the sample quenched at 0.03 s showed ~30% decrease of the SfaA•Fe(II)•2OG•5-$^2H_2$-**1** complex with the simultaneous accumulation of a species with parameters of δ = 0.31 mm/s and ΔE_Q = 0.59 mm/s, representing ~20% of the total iron. This new species is similar to the ferryl intermediate observed in other Fe/2OG enzymes.[5b, 9] In addition, a minor ferrous species with parameters of δ = 1.25 mm/s and ΔE_Q = 1.90 mm/s (~13% of the iron in the sample) was also observed. This ferrous species was more readily accumulated in the sample quenched at 0.03 s when **1** was used, which represented ~ 25% of the total iron. We tentatively assign this ferrous species as a potential product complex. Importantly, compared to the reaction using 5-$^2H_2$-**1**, the sample quenched at 0.03 s using **1** did not show a significant accumulation of the ferryl intermediate (< 5%). Thus, accumulation of the ferryl species using 5-$^2H_2$-**1** is likely due to the kinetic isotope effect from the replacement of the targeted C5-H bond with the C5-D bond. Overall, Mössbauer analysis suggests that the initial C-H activation by the ferryl intermediate occurs at the C5 position of **1**.

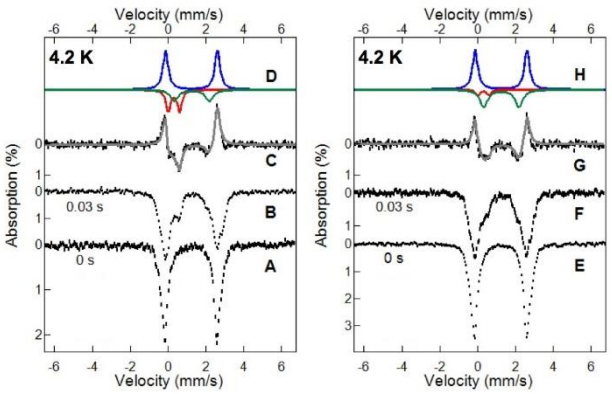

Figure 3. The Mössbauer spectra of SfaA•Fe(II)•2OG•5-$^2H_2$-**1** and SfaA•Fe(II)•2OG•**1** are shown in A and E; The spectra of the samples quenched at 0.03 s are shown in B and F; The difference spectra between A and B (B-A), E and F (F-E), and the spectral simulations (grey lines) are shown in C and G, which indicate the decrease of the quaternary complex (upward blue simulations), the accumulation of the ferryl intermediate (the red simulations) and the additional ferrous species (the green simulations in D and H). See Table S1-S3 for details simulation parameters.

In the structure of ScoE•Fe•**3**, the C5 of **3** moves ~0.4 Å closer to the iron center (4.9 → 4.5 Å from ScoE•Fe•**3** to ScoE•Fe•**1**). However, the orientation of **3** is probably not at optimal position for H• abstraction where the C5-H is not pointing toward the iron. Meanwhile, the N atom located ~5.9 Å away from the iron center may also not be properly positioned to interact with the iron

Accepted Manuscript

This article is protected by copyright. All rights reserved.

(Figure 1C, Figure S22). To reveal possible pathway involved in the second reaction, the proposed intermediates **4** and **6** were synthesized. As shown in Scheme 2, pathway *i*, followed by hydroxylation at the C5 position of **4**, **5**, which likely tautomerizes to **6** rapidly, may proceed through dehydration/decarboxylation to produce **2**. Alternatively, second hydroxylation of **3** will produce **6** through the proposed intermediate **7**. After incubating enzyme, Fe, 2OG, O_2 and cis-**4**, the reactions were analyzed by LC-MS. Under the current conditions, no production of **2** can be detected. When **6** was tested with enzyme under anoxic conditions or in the presence of 2OG and O_2, production of **2** was not observed (Figure S18). Although it is possible that cis-**4** or **6** cannot enter the active site, or the trans-**4** serves as the actual intermediate, these results imply the pathway involving **4** or **6** is less likely and suggest that the alternative pathway may be utilized (pathway *ii*) where isonitrile formation possibly involves a reactive iron species assisted decarboxylation. Namely, during the second reaction, the presumptive ferryl species is used to trigger decarboxylation by activating the N and the reaction is then followed by dehydration (**3** → **8** → **2**). Alternatively, subsequent to dehydration of **3**, an analogous decarboxylation will result in protonated isonitrile (**9**). Although it is less common, desaturation via oxidative decarboxylation has been reported in several Fe/2OG enzymes catalyzed olefination.[10] In addition, N-hydroxylation was reported in a non-heme iron enzyme catalyzed reaction in streptozotocin biosynthesis.[11]

In short, in studying three Fe/2OG enzyme catalyzed isonitrile installation, the experimental analyses establish that isonitrile formation goes through two consecutive, but distinctive, reactions. In the first reaction, an Fe(IV)-oxo species is utilized to generate C5-hydroxylated product (**3**). Conversion of **3** to **2** likely proceeds by decarboxylation-assisted desaturation. Although the detailed mechanism remains to be evaluated, these observations enrich our view in diverse strategies that Fe/2OG enzymes used to catalyze novel reactions. Considering the conserved biosynthetic approach used to install the isonitrile-containing peptides found in several pathogenic bacteria, these observations may shed light for development of new anti-virulence therapeutics target for bacterial infection.

Acknowledgements

This work was supported by North Carolina State University, Carnegie Mellon University, grants from the National Key Research and Development Program of China (2018YFA0901900 to J.Z.), Shanghai Municipal Science and Technology Commission (19XD1404800 to J.Z.), and the National Institutes of Health (GM127588 to W.-c. C., and Y. G.). We thank the staffs in beamline BL17U1 and BL19U1 of Shanghai Synchrotron Radiation Facility for help in data collection. We also thank Prof. Jianhua Gan for his help in structure refinement.

Author Contributions

†These authors contributed equally.

Keywords: Fe/2OG enzyme • isonitrile • enzyme mechanism • decarboxylation • catalysis

[1] a) L. J. Wang, M. Y. Zhu, Q. B. Zhang, X. Zhang, P. L. Yang, Z. H. Liu, Y. Deng, Y. G. Zhu, X. S. Huang, L. Han, S. Q. Li, J. He, *ACS Chem. Biol.* **2017**, *12*, 3067-3075; b) J. M. Crawford, C. Portmann, X. Zhang, M. B. J. Roeffaers, J. Clardy, *Proc. Natl. Acad. Sci. U.S.A.* **2012**, *109*, 10821-10826; c) S. Y. Mo, A. Krunic, G. Chlipala, J. Orjala, *J. Nat. Prod.* **2009**, *72*, 894-899; d) M. F. Clarke-Pearson, S. F. Brady, *J. Bacteriol.* **2008**, *190*, 6927-6930; e) S. F. Brady, J. Clardy, *Angew. Chem. Int. Ed. Engl.* **2005**, *44*, 7063-7065; f) M. J. Garson, J. S. Simpson, *Nat. Prod. Rep.* **2004**, *21*, 164-179; g) K. Stratmann, R. E. Moore, R. Bonjouklian, J. B. Deeter, G. M. L. Patterson, S. Shaffer, C. D. Smith, T. A. Smitka, *J. Am. Chem. Soc.* **1994**, *116*, 9935-9942; h) W. L. Parker, M. L. Rathnum, J. H. Johnson, J. S. Wells, P. A. Principe, R. B. Sykes, *J. Antibiot.* **1988**, *41*, 454-460; i) C. W. J. Chang, A. Patra, D. M. Roll, P. J. Scheuer, G. K. Matsumoto, J. Clardy, *J. Am. Chem. Soc.* **1984**, *106*, 4644-4646.

[2] a) W.-c. Chang, D. Sanyal, J. L. Huang, K. Ittiamornkui, Q. Zhu, X. Liu, *Org. Lett.* **2017**, *19*, 1208-1211; b) S. F. Brady, J. Clardy, *Angew. Chem. Int. Ed. Engl.* **2005**, *44*, 7045-7048.

[3] a) N. C. Harris, D. A. Born, W. L. Cai, Y. B. Huang, J. Martin, R. Khalaf, C. L. Drennan, W. J. Zhang, *Angew. Chem. Int. Ed. Engl.* **2018**, *57*, 9707-9710; b) N. C. Harris, M. Sato, N. A. Herman, F. Twigg, W. L. Cai, J. Liu, X. J. Zhu, J. Downey, R. Khalaf, J. Martin, H. Koshino, W. J. Zhang, *Proc. Natl. Acad. Sci. U.S.A.* **2017**, *114*, 7025-7030.

[4] a) M. S. Islam, T. M. Leissing, R. Chowdhury, R. J. Hopkinson, C. J. Schofield, *Annu. Rev. Biochem.* **2018**, *87*, 585-620; b) S. S. Gao, N. Naowarojna, R. Cheng, X. Liu, P. Liu, *Nat. Prod. Rep.* **2018**, *35*, 792-837; c) S. Martinez, R. P. Hausinger, *J. Biol. Chem.* **2015**, *290*, 20702-20711; d) J. M. Bollinger, Jr.;, W.-c. Chang, M. L. Matthews, R. J. Martinie, A. K. Boal, C. Krebs, in *2-Oxoglutarate-Dependent Oxygenases* (Eds.: R. P. Hausinger, C. J. Schofield), Royal Society of Chemistry **2015**, pp. 95-122.

[5] a) J. C. Price, E. W. Barr, B. Tirupati, J. M. Bollinger, Jr., C. Krebs, *Biochemistry* **2003**, *42*, 7497-7508; b) J. C. Price, E. W. Barr, T. E. Glass, C. Krebs, J. M. Bollinger, Jr., *J. Am. Chem. Soc.* **2003**, *125*, 13008-13009.

[6] R. P. Hausinger, in *2-Oxoglutarate-Dependent Oxygenases* (Eds.: R. P. Hausinger, C. J. Schofield), Royal Society of Chemistry, **2015**, pp. 1-58.

[7] S. Omura, H. Ikeda, J. Ishikawa, A. Hanamoto, C. Takahashi, M. Shinose, Y. Takahashi, H. Horikawa, H. Nakazawa, T. Osonoe, H. Kikuchi, T. Shiba, Y. Sakaki, M. Hattori, *Proc. Natl. Acad. Sci. U.S.A.* **2001**, *98*, 12215-12220.

[8] a) W.-c. Chang, Y. Guo, C. Wang, S. E. Butch, A. C. Rosenzweig, A. K. Boal, C. Krebs, J. M. Bollinger, Jr., *Science* **2014**, *343*, 1140-1144; b) N. P. Dunham, W.-c. Chang, A. J. Mitchell, R. J. Martinie, B. Zhang, J. A. Bergman, L. J. Rajakovich, B. Wang, A. Silakov, C. Krebs, A. K. Boal, J. M. Bollinger, Jr., *J. Am. Chem. Soc.* **2018**, *140*, 7116-7126; c) A. J. Mitchell, N. P. Dunham, J. A. Bergman, B. Wang, Q. Zhu, W.-c. Chang, X. Liu, A. K. Boal, *Biochemistry* **2017**, *56*, 441-444.

[9] W.-c. Chang, J. Li, J. L. Lee, A. A. Cronican, Y. Guo, *J. Am. Chem. Soc.* **2016**, *138*, 10390-10393.

[10] a) C. P. Yu, Y. Tang, L. Cha, S. Milikisiyants, T. I. Smirnova, A. I. Smirnov, Y. Guo, W.-c. Chang, *J. Am. Chem. Soc.* **2018**, *140*, 15190-15193; b) J. Zhu, G. M. Lippa, A. M. Gulick, P. A. Tipton, *Biochemistry* **2015**, *54*, 2659-2669; c) J. L. Huang, Y. Tang, C. P. Yu, D. Sanyal, X. Jia, X. Liu, Y. Guo, W.-c. Chang, *Biochemistry* **2018**, *57*, 1838-1841.

[11] a) T. L. Ng, R. Rohac, A. J. Mitchell, A. K. Boal, E. P. Balskus, *Nature* **2019**, *566*, 94-99; b) H. Y. He, A. C. Henderson, Y. L. Du, K. S. Ryan, *J. Am. Chem. Soc.* **2019**, *141*, 4026-4033.

Accepted Manuscript

This article is protected by copyright. All rights reserved.

10.1002/anie.201914896

WILEY-VCH

COMMUNICATION

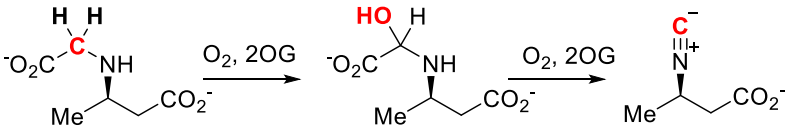

A subclass of Fe/2OG enzyme catalyzes decarboxylation-assisted desaturation of N-alkyl glycine to install the isonitrile functionality. By using a complementary approach including structure determination, NMR, and Mössbauer analyses, the reaction intermediate and plausible reaction mechanism is established.

WILEY-VCH

Accepted Manuscript

This article is protected by copyright. All rights reserved.